Molecular Crystals and Liquid Crystals
Publication details, including instructions for authors and subscription information:
http://www.tandfonline.com/loi/gmcl20

Laser Surface Alloying of Aluminium AA1200

L. A. B. Mabhali [a b], S. L. Pityana [a c] & N. Sacks [b]

[a] CSIR National Laser Centre, Pretoria, Republic of South Africa

[b] Department of Chemical and Metallurgical Engineering, University of the Witwatersrand, Johannesburg, Republic of South Africa

[c] Department of Chemical and Metallurgical Engineering, Tshwane University of Technology, Pretoria, South Africa

Available online: 14 Feb 2012

To cite this article: L. A. B. Mabhali, S. L. Pityana & N. Sacks (2012): Laser Surface Alloying of Aluminium AA1200, Molecular Crystals and Liquid Crystals, 555:1, 138-148

To link to this article: http://dx.doi.org/10.1080/15421406.2012.635095

Mol. Cryst. Liq. Cryst., Vol. 555: pp. 138–148, 2012

ISSN: 1542-1406 print/1563-5287 online
DOI: 10.1080/15421406.2012.635095

Taylor & Francis
Taylor & Francis Group

Laser Surface Alloying of Aluminium AA1200

L. A. B. MABHALI,[1,2,*] S. L. PITYANA,[1,3] AND N. SACKS[2]

[1]CSIR National Laser Centre, Pretoria, Republic of South Africa
[2]Department of Chemical and Metallurgical Engineering, University of the Witwatersrand, Johannesburg, Republic of South Africa
[3]Department of Chemical and Metallurgical Engineering, Tshwane University of Technology, Pretoria, South Africa

Aluminium AA1200 was laser alloyed with mixtures of Ni, Ti and SiC powders using a 4.4 kW Rofin Sinar Nd:YAG laser to improve its surface hardness. The reactions of Al with Ni resulted in the in situ formation of Al_3Ni and Al_3Ni_2 intermetallic phases while Ti reacted with Al to form an Al_3Ti. Some of the SiC particles dissociated and reacted with either Al or Ti to form Al_4C_3, Al_4SiC_4, TiC or Ti_3SiC_2 phases. Si reacted with Ti to form a Ti_5Si_3 phase. Surface hardness increased after laser alloying due to the formation of intermetallic phases and metal matrix composites.

Keywords Laser alloying; metal matrix composites; intermetallic phases; aluminium

Introduction

Low hardness and wear resistance of aluminium alloys restrict its use especially in applications where good surface properties are required. The tribological properties of materials are determined by the surface condition; hence it is usual to enhance a materials wear resistance by means of surface modification. Laser surface alloying is one of the techniques used for this purpose [1–3]. In laser surface alloying, alloying powders are mixed into the laser generated molten pool on the surface of a material. On solidification, an alloyed surface layer is formed. The microstructure of the alloyed layer usually contains intermetallic compounds (IC). In addition to the IC, hard particles can also be added to the melt pool resulting in metal matrix composite (MMC) surfaces. By varying the process parameters such as laser power, beam spot size, laser scan speed and powder feed rate a good composition and particle distribution can be achieve in the alloyed layer.

Laser alloying of aluminium AA1100 with electrodeposited nickel was performed by Selvan et al. [4] using a CO_2 laser. Alloying was performed with a beam diameter of 1 mm for various scanning speeds and laser powers. The intermetallic phases formed were Al_3Ni and Al_3Ni_2. These phases were also observed by other authors [5,6]. The hardness of the alloyed layers was in the range of 600–950 $HV_{0.1}$. Wendt et al. [7] laser alloyed aluminium with a titanium wire using CO_2 and Nd:YAG lasers. The microstructure of the alloyed layer consisted of a Ti-supersaturated Al matrix and $TiAl_3$ intermetallic phase. When the substrate was an Al-Si alloy, the intermetallic phase $Ti(Al,Si)_3$ was formed. Man et al. [8] used a continuous wave Nd:YAG laser to alloy aluminium AA6061 with preplaced NiTi (54 wt%

*Address correspondence to L. A. B. Mabhali, CSIR National Laser Centre, Pretoria, Republic of South Africa. E-mail: lmabhali@yahoo.com

Ni & 46 wt% Ti) powder to improve its hardness and wear resistance. The intermetallic phases observed after laser alloying were dendrites of $TiAl_3$ and Ni_3Al. The interdendritic film was composed of α-Al. A hardness increase of 200 HV and wear resistance of about 5.5 times that of the virgin substrate was achieved for the modified layer. The increase in hardness and wear resistance was attributed to the formation of the $TiAl_3$, Ni_3Al and α-Al phases. Ternary intermetallic phases were not reported by the authors. Mabhali et al. [9] observed Al_3Ni, Al_3Ni_2, Al_3Ti and NiTi intermetallic phases when laser alloying aluminium AA1200 with Ni and Ti powders of different compositions. A hardness increase of up to 808 HV was achieved after alloying with 80 wt% Ni and 20 wt% Ti. The authors reported that the hardness and wear resistance increased as the Ni content in the alloying powder increased.

Various researchers have studied the phases formed when aluminium was laser alloyed with SiC [10–14]. The common observation was that the phases are temperature dependent. When the alloying temperatures are between 940–1620 K, the brittle Al_4C_3 phase is formed by the reaction $4Al + 3SiC \rightarrow Al_4C_3 + 3Si$. At temperatures above or equal to 1670 K, the Al_4SiC_4 phase is formed by the reaction $4Al + 4SiC \rightarrow Al_4SiC_4 + 3Si$. The presence of the Al_4C_3 phase in MMC is not desirable as it is brittle and hydroscopic. Work has been conducted to suppress the formation of the Al_4C_3 phase during laser processing. Su and Lei [12] laser cladded Al-12 wt% Si with a powder containing SiC and Al-12 wt% Si in a 3:1 volume ratio. The addition of Al-12 wt% Si was found to suppress or eliminate the aluminium carbides in the MMC layer. A good distribution of injected SiC particles was achieved near the surface. The microhardness of the coating was between 220 and 280 HV. Leòn and Drew [15] coated SiC with Ni to improve their wettability by liquid Al. Coating SiC with Ni increased the overall surface energy of the solid, promoting wetting by the liquid aluminium and the Al/SiC adhesion which led to the suppression of aluminium carbide formation [15,16]. The Al_3Ni and Al_3Ni_2 intermetallic phases were formed from the reaction of aluminium with nickel. The exothermic nature of the Ni-Al interaction together with the precipitation of the Al_3Ni and Al_3Ni_2 intermetallic phases were the reported factors leading to the improvement of the wettability of SiC by aluminium.

Kloosterman et al. [17] laser injected SiC particles into a Ti-6Al-4V alloy. At high temperatures, SiC decomposed and the C reacted with Ti to form TiC dendrites. These TiC dendrites were randomly orientated and distributed over the alloyed track. TiC was also observed around the SiC particles as either a cellular reaction layer or an irregular reaction layer. These reaction layers were also observed by Pei et al. [18]. The cellular layer was relatively thin and regularly shaped around the SiC particles. Spherical TiC grains were formed in the irregular layer with a ternary Ti_3SiC_2 phase found as small plates around the randomly orientated spherical TiC grains. This Ti_3SiC_2 phase was also confirmed by other authors [19–21]. The microstructure of the matrix consisted of α-Ti and Ti_5Si_3 eutectic phases. Ti_5Si_3 is the more thermodynamically stable phase in the Si-Ti phase diagram [22,23]. Other titanium silicides (Ti_3Si and Ti_5Si_4) are unstable especially in the presence of carbon and play a minor role in the Al-C-Si-Ti system [20]. The hardness of the alloyed layer was between 650 and 1100 HV. Li et al. [24] reported the formation of TiC and Ti_5Si_3 when Ti reacts with SiC and when the temperature is between 1173 and 1373 K, while Ti_3SiC_2 phase is formed above 1473 K. Man et al. [25] synthesized TiC in situ on an AA6061 aluminium surface by alloying with SiC and Ti powders. The optimum powder composition for a high quality surface metal matrix composite was achieved with 40 wt% SiC and 60 wt% Ti. XRD analysis of the alloyed layer revealed TiC, TiAl, Ti_3Al, SiC, Al and Si phases. The hardness increased from 75 HV to 650 HV due to the formation of the TiC particles and TiAl and Ti_3Al intermetallics.

This work investigates the microstructure and hardness of aluminium AA1200 laser alloyed with different mixtures of Ni, Ti and SiC powders. A comparison of the effect of IC, MMC and a mixture of both (IC and MMC) on the hardness of the alloys was investigated.

Experimental

The laser surface alloying-particle injection was carried out using a high power continuous wave Nd:YAG laser. The laser beam was guided by an optical fibre of 400 microns in diameter. In these experiments, the laser beam spot size was fixed to 4 mm in diameter. A KUKA robot was used to deliver the laser beam to the target substrate. The applied laser power was 4 kW and the laser scan speed was varied between 10 and 20 mm/s. An off axis nozzle of 2.5 mm in diameter was used for powder delivery. The nozzle was mounted on the laser head and fixed at a distance of 12 mm from the substrate. This arrangement assured that the powder stream coincided with the laser beam at the interaction zone. The starting powders used were Ni, Ti and SiC. These were mixed together in different weight ratios. Table 1 shows the ratios of the stating powders. The mixed powders were fed into the melt pool by means of an argon gas carrier. A commercial powder feed instrument equipped with a flow balance was used for controlling the powder feed rate which was set to 2 g/min. In order to avoid oxidation argon gas was used for shielding the laser-substrate and powder interaction zone.

The substrate material was a commercially pure aluminium AA1200 metal. Its nominal chemical composition is 0.12 wt% Cu, 0.13 wt% Si, 0.59 wt% Fe and the rest was Al. The working samples were cut to 100 mm $\times$ 100 mm plates of 6 mm thickness. Prior to laser processing, the surfaces of the aluminium plates were sand blasted and cleaned with acetone. This was done in order to enhance the absorption of laser radiation by the target surface.

After laser alloying cross-sections of the samples were prepared for metallurgical examination. The mechanically polished surfaces were etched with Kellers's reagent. An OLYMPUS BX51M optical microscope and a Leo 1525 scanning electron microscope (SEM) equipped with an energy dispersive X-ray (EDX) system were used for microstructure investigations. The EDX was used for elemental analysis. The phases in the layer were

Table 1. Starting powder mixtures

Sample number	Composition
1	100 wt% Ni
2	100 wt% Ti
3	100 wt% SiC
4	50 wt% Ni + 50 wt% Ti
5	50 wt% Ni + 50 wt% SiC
6	50 wt% Ti + 50 wt% SiC
7	20 wt% Ni + 30 wt% Ni + 50 wt% SiC
8	33.3 wt% Ni + 33.3 wt% Ni + 33.3 wt% SiC
9	50 wt% Ni + 30 wt% Ti + 20 wt% SiC
10	80 wt% Ni + 15 wt% Ti + 50 wt% SiC

identified by X-ray diffraction (XRD) using a P Analytical X′Pert Pro powder diffractometer with an X′Celerator detector. The radiation source used was CuK_α. The phases were indexed using X′Pert High-score Plus software. The surface hardness of the untreated aluminium metal and the laser alloyed samples was determined using a Matsuzawa hardness tester with a load of 100 g.

Results and Discussion

Laser alloying aluminium with Ni, Ti and SiC was performed successfully and the laser scanning speed for optimum parameters was determined as 10 mm/s. This scanning speed resulted in homogeneous surfaces free of cracks and porosity. Intermetallic phases were formed in-situ due to reactions between metallic materials (e.g. Al with Ni and/or Ti) while metal matrix composites were formed due to the injection of ceramics (e.g. SiC) during laser alloying.

Laser alloying of aluminium AA1200 with Ni only resulted in the formation of an α-Al (black) matrix and an Al_3Ni_2 (grey) intermetallic phase as shown in Fig. 1(a). The Al_3Ni_2 intermetallic phase was formed in-situ by the reaction of Al and Ni. The Al_3Ni_2 phase was also reported by various authors [5,6,26]. The Al_3Ti intermetallic phase shown in Fig. 1(b) was formed in-situ due to the reaction of Al with Ti. This phase was also observed by Wendt et al. [7]. The matrix consisted of an Al-Ti eutectic phase. The phases were confirmed by XRD as shown in Figs. 2(a) and 2(b).

Laser alloying of aluminium with the SiC powders resulted in the formation of a metal matrix composite reinforced with SiC particles. The microstructure of the laser alloyed layer is shown in Fig. 3(a) and its XRD in Fig. 3(b). Due to the high temperatures (2362°C) generated during laser alloying, some of the SiC particles dissociated to form Si and C. Al reacted with Si and C to form the Al_4SiC_4 phase. It has been reported [12–14] that the temperature required for this reaction to occur is above or equal to 1670 K. The free Si (white phases) produced during this reaction is observed in Fig. 3(a). The Al_4C_3 phase which forms at temperatures between 940–1620 K was not observed. This indicates that the temperature of the melt pool was above 1620 K. The matrix consisted of α-Al and Al-Si eutectic phases. The retained SiC particles formed the MMC.

The microstructure of aluminium AA1200 laser alloyed with 50wt% Ni + 50wt% Ti is shown in Fig. 4(a) and the XRD diffractograph in Fig. 4(b). The intermetallic phases,

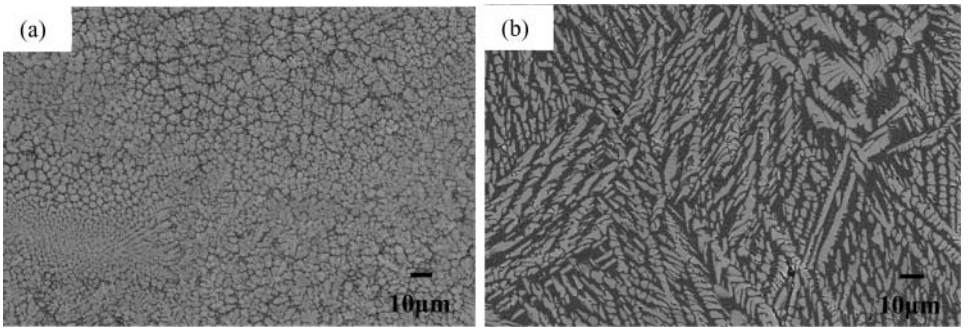

Figure 1. SEM micrograph of Al AA1200 laser alloyed with (a) Ni powder showing an in-situ formed Al_3Ni_2 phase (grey) within an α-Al (black) matrix and (b) Ti powder showing α-Al (black) and Al_3Ti (grey) phases.

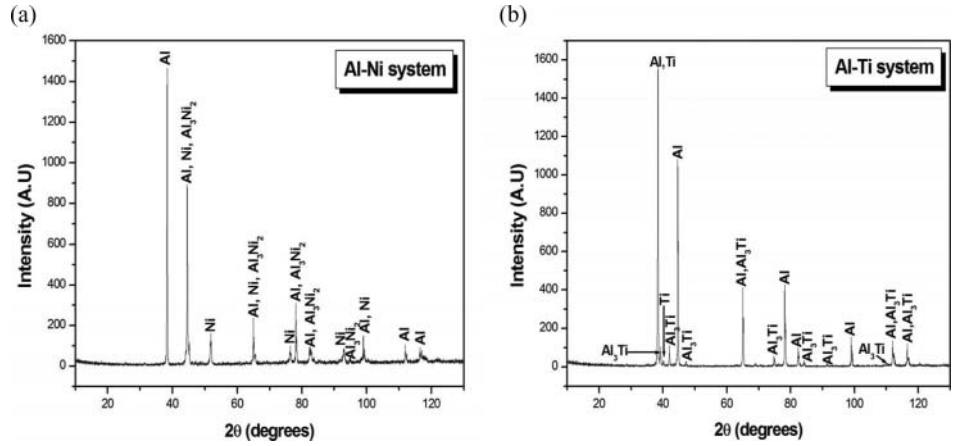

Figure 2. XRD of Al laser alloyed with (a) Ni and (b) Ti.

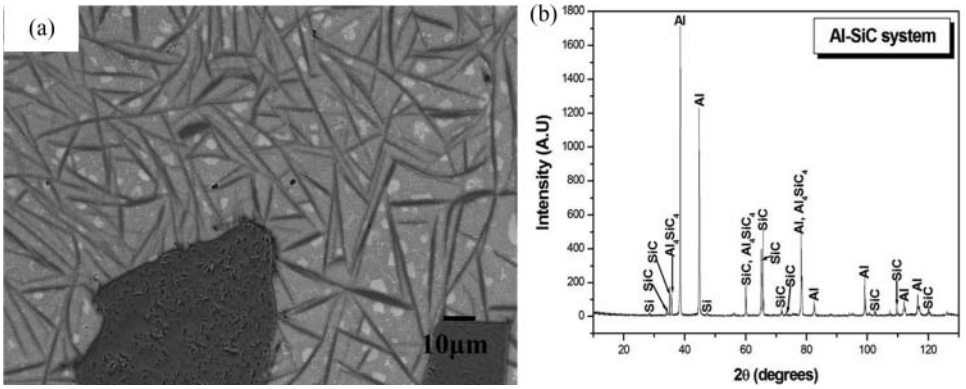

Figure 3. (a) SEM micrograph of an Al laser alloyed with SiC powder showing SiC particle (black particle), Al_4SiC_4 intermetallic phase (dark grey platelets), Si phase (white), α-Al (grey) and Al-Si eutectic phase (white dots in the grey phase). (b) XRD of Al laser alloyed with SiC.

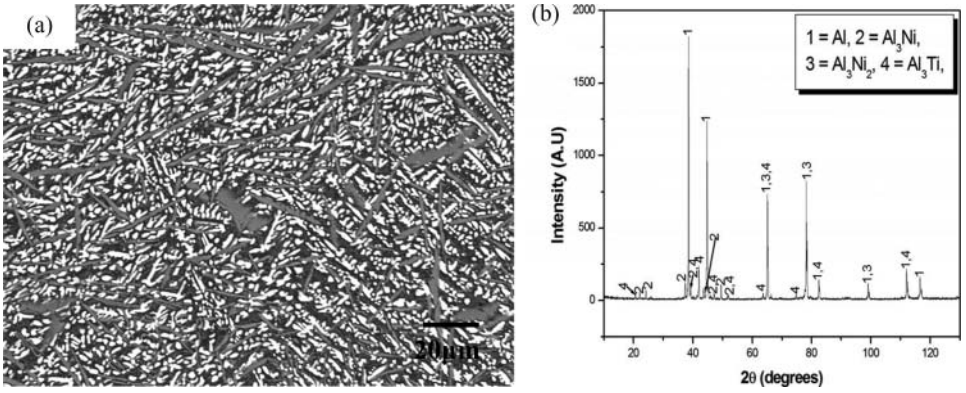

Figure 4. (a) SEM micrograph of an Al laser alloyed with 50 wt% Ni + 50 wt% Ti showing Al_3Ni phase (white), Al_3Ti phase (grey), and α-Al (black). (b) XRD of Al laser alloyed with 50 wt% Ni + 5-wt% Ti.

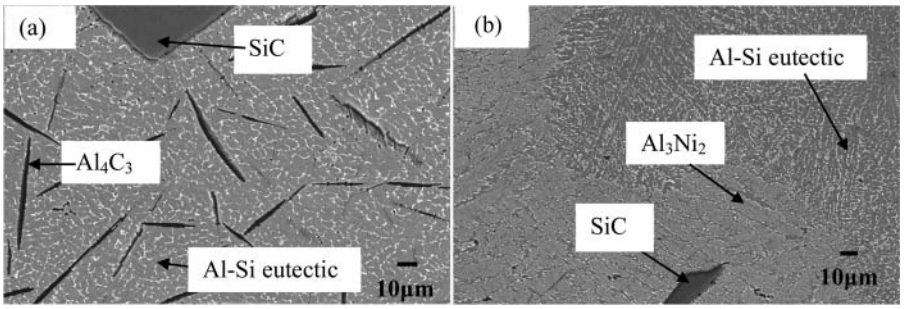

Figure 5. SEM micrograph of an Al laser alloying with 50 wt% Ni + 50 wt% SiC showing (a) SiC particle, Al_4C_3 intermetallic phase, α-Al (grey) and Al-Si eutectic phase (white phase in the grey α-Al phase); and (b) Al_3Ni_2 intermetallic phase, Al_3Ni intermetallic phase (white phase around Al_3Ni_2) and Al-Si eutectic phase.

formed in-situ, were Al_3Ni, Al_3Ni_2 and Al_3Ti. The phases were formed due to the reactions of Al with Ni and Ti respectively.

To determine the combined effect of intermetallic phases and metal matrix composites, aluminium was laser alloyed with mixed Ni + SiC powders and mixed Ti + SiC powders. Laser alloying aluminium AA1200 with 50 wt% Ni + 50 wt% SiC resulted in the microstructures shown in Fig. 5. SiC particles, an Al_3Ni_2 phase and an Al-Si eutectic were observed in the microstructures. The Al_3Ni phase was observed around the Al_3Ni_2 phase. This intermetallic phase formed in situ as a peritectic product of a reaction between liquid Al and the Al_3Ni_2 phase. Due to the high temperatures reached in the alloyed layer, some of the SiC particles dissociated and reacted with Al to form a needle-like Al_4C_3 phase. An Al_3Ni phase was formed from the reaction of Al with Ni. The retained SiC particles formed a MMC. The phases were identified with the XRD in Fig. 6.

Figure 7 shows the microstructure of aluminium AA1200 laser alloyed with 50 wt% Ti + 50 wt% SiC. The phases observed in the microstructure were Al, SiC, TiC, Ti_5Si_3 and Al_3Ti and these phases are shown in the XRD in Fig. 8. Due to the high laser alloying temperatures, some of the SiC particles dissociated and reacted with Ti to form Ti_5Si_3 and

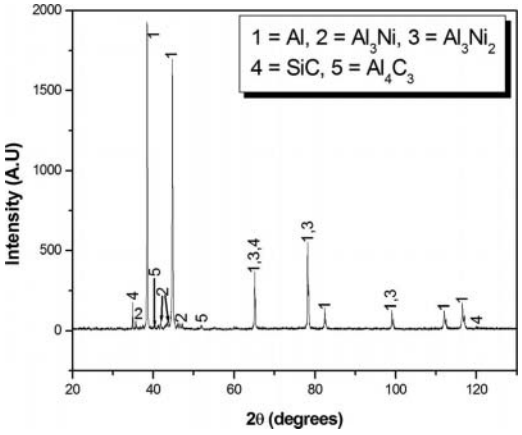

Figure 6. XRD of Al laser alloyed with 50 wt% Ni + 50 wt% SiC.

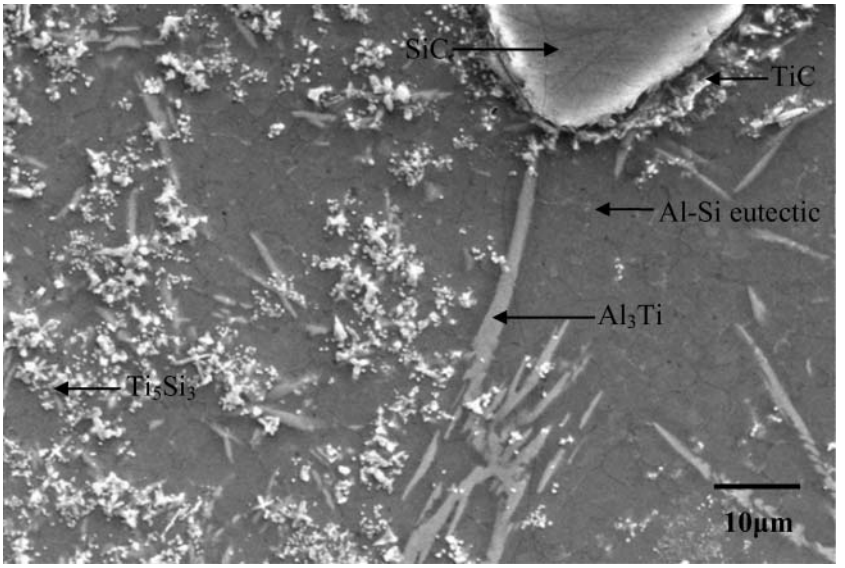

Figure 7. Micrographs of an Al laser alloyed with 50 wt% Ti + 50 wt% SiC showing SiC, Al-Si eutectic, TiC, Al_3Ti and Ti_5Si_3.

TiC. The Ti_5Si_3 phase is the most stable phase in the Ti-Si system as it has the lowest energy of formation [27]. Al reacted with Ti to form the Al_3Ti intermetallic phase. The interfacial TiC phase was formed around the SiC particles due to adsorption of Ti on the SiC particle surface. The retained SiC particles formed a MMC. The matrix consists of α-Al and Al-Si eutectic.

Laser alloying Al with Ni, Ti and SiC simultaneously resulted in the formation of metal matrix composites (reinforced with SiC) and intermetallic phases. SEM micrographs of surfaces laser alloyed with different ratios of Ni, Ti and SiC are shown in Fig. 9 and their phases shown in the XRD in Fig. 10. Due to different densities, Ni ($\rho = 8.91$ g/cm^3),

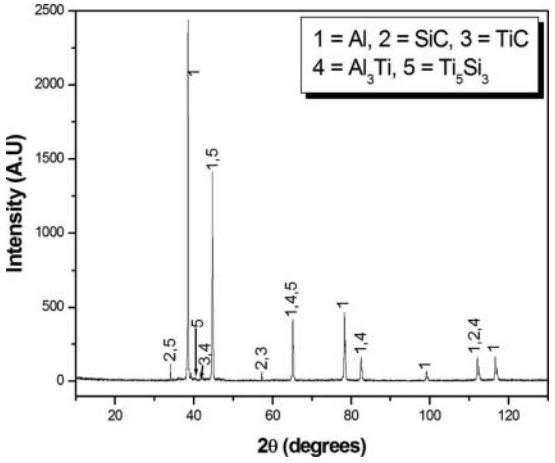

Figure 8. XRD of Al laser alloyed with 50 wt% Ti + 50 wt% SiC.

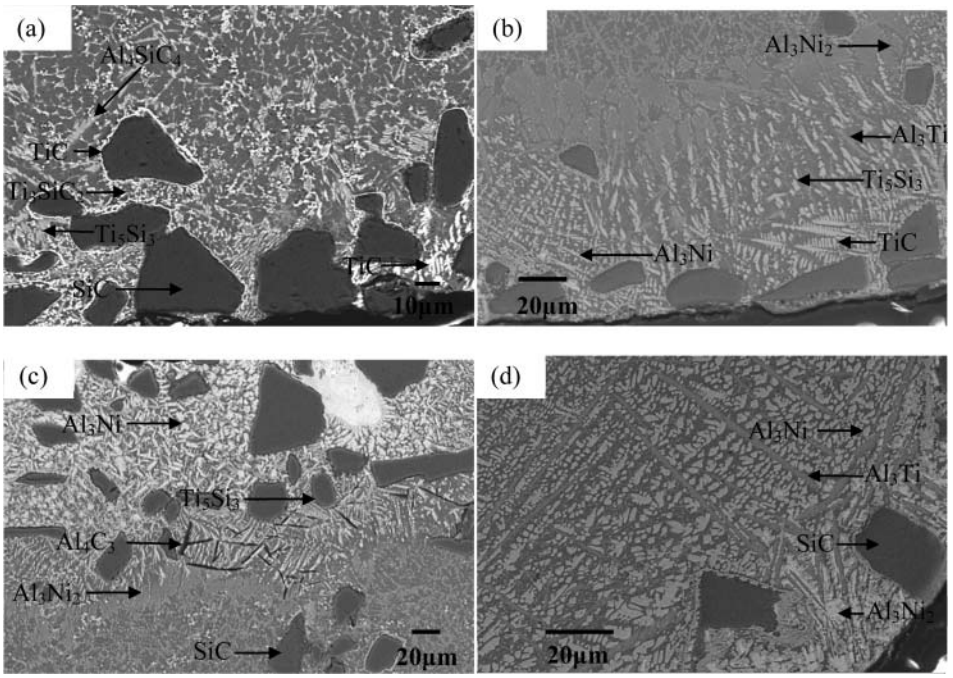

Figure 9. Micrographs of an Al laser alloyed with (a) 20 wt% Ni + 30 wt% Ti + 50 wt% SiC, (b) 33.3 wt% Ni + 33.3 wt% Ti + 33.3 wt% SiC, (c) 50 wt% Ni + 20 wt% Ti + 30 wt% SiC, (d) 80 wt% Ni + 15 wt% Ti + 5 wt% SiC.

Ti ($\rho = 4.51$ g/cm^3) and SiC ($\rho = 3.21$ g/cm^3) reacted with the Al at different positions within the alloyed layer. Generally the SiC reacted with molten Al close to the surface while Ni reacted with Al near the middle of the alloyed layer. The needle-like Al_3Ti phase was observed throughout the microstructure. Two types of Al_3Ni phases were observed. The dendritic Al_3Ni phase was produced from a eutectic reaction between Ni and liquid Al, while the Al_3Ni phase observed around the Al_3Ni_2 phase was produced as a peritectic product of a reaction between liquid Al and the Al_3Ni_2 phase. The equiaxed dendritic Al_3Ni_2 phase which is enveloped by the Al_3Ni phase is observed in Fig. 9(b). Due to the high Al content in the base material compared to the Ti and Ni contents, only the Al-rich intermetallic phases were observed [5,28]. Due to the high surface temperatures achieved during laser alloying, some of the SiC powder particles dissolved in the melt pool. The dissolved SiC particles dissociated to form Si and C. The C reacts with either Ti or Al to form TiC or the brittle Al_4C_3 phase. The Gibbs free energy is more negative for the formation of TiC and thus there was a higher tendency for the formation of TiC than for Al_4C_3 [25]. Two types of TiC phases were observed, namely dendritic and interfacial TiC as indicated in Fig. 9(b). The interfacial TiC phases were formed around SiC particles due to adsorption of Ti on the SiC surface. Due to the high cooling rates associated with laser treatment, these TiC phases did not grow or aggregate. The dendritic TiC phases were formed inside the melt pool from the reaction of the dissolved SiC particles and Ti. The free Si (from SiC) reacted with Ti to form Ti_5Si_3. This is a thermodynamically favourable phase and has the lowest Gibbs free energy compared to other Ti-Si phases such as TiSi, $TiSi_2$ and Ti_5Si_4 [27]. Traces of Ti_3SiC_2 and Al_4SiC_4 were also detected in the XRD of

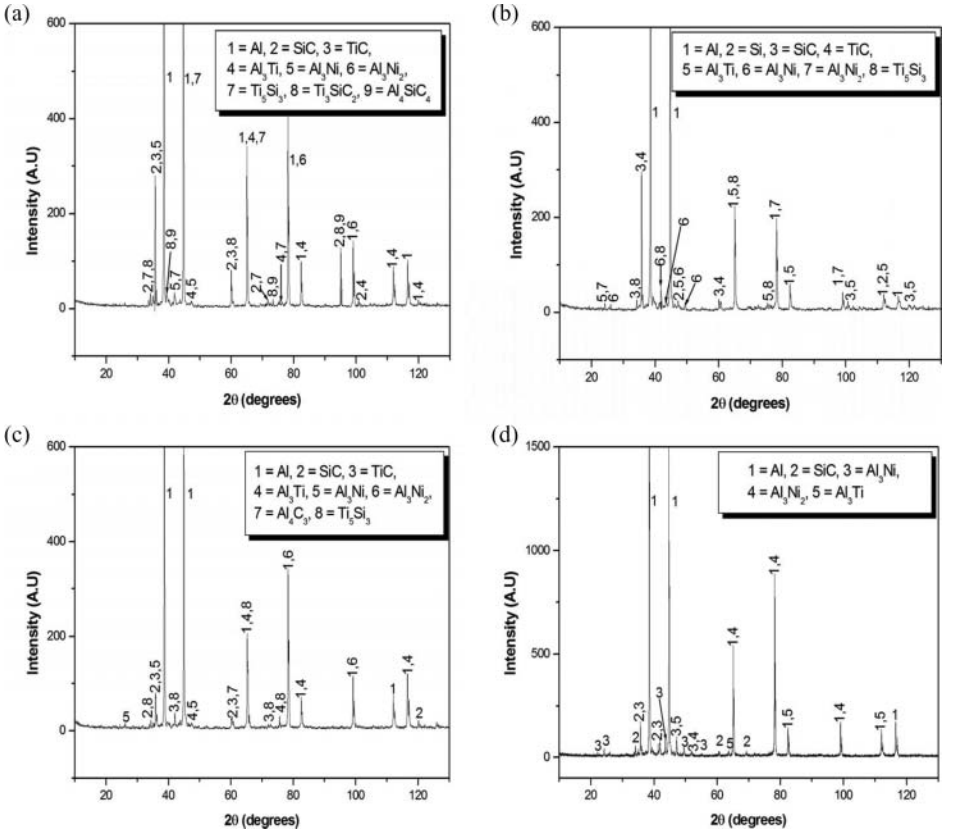

Figure 10. XRD of Al laser alloyed with (a) 20 wt% Ni + 30 wt% Ti + 50 wt% SiC, (b) 33.3 wt% Ni + 33.3 wt% Ti + 33.3 wt% SiC, (c) 50 wt% Ni + 20 wt% Ti + 30 wt% SiC, (d) 80 wt% Ni + 15 wt% Ti + 5 wt% SiC.

surfaces laser alloyed with high Ti and SiC contents (viz. 20 wt% Ni + 30 wt% Ti + 50 wt% SiC).

The hardness results for the untreated aluminium AA1200 and the laser alloyed surfaces are show in Table 2. The results show that laser alloying improved the surface hardness for all the compositions used compared to the pure aluminium AA1200 metal. The increase in hardness was attributed to the formation of the intermetallic phases in the laser alloyed surfaces. Grain refinement, due to the rapid heating and cooling rates associated with laser alloying plays a role in increasing the hardness of the laser alloyed surfaces [29]. The highest hardness of 766.9 ± 38.5 HV was achieved when laser alloying with Ni only. This high hardness was attributed to the equiaxed dendritic Al_3Ni_2 phase. The high density of this phase results in small Al mean free paths between the grains and this limits the contribution of the pure aluminium to the hardness of the high Ni alloys. The needle-like Al_3Ti resulted in large Al mean free paths between the grains which lowered the surface hardness, while the Si containing intermetallic phases namely, Ti_5Si_3, Ti_3SiC_2 and Al_4SiC_4 did not affect the hardness significantly due to the low volume fraction of these phases.

Table 2. Hardness

Composition	Hardness ($HV_{0.1}$)
Aluminium AA1200	24.0 ± 0.4
100 wt% Ni	766.9 ± 38.5
100 wt% Ti	159.2 ± 17.5
100 wt% SiC	238.3 ± 33.7
50 wt% Ni + 50 wt% Ti	220 ± 14.7
50 wt% Ni + 50 wt% SiC	110 ± 10.4
50 wt% Ti + 50 wt% SiC	111.3 ± 20.3
20% Ni + 30 wt% Ti + 50 wt% SiC	152.1 ± 21.4
33.3 wt% Ni + 33.3 wt% Ti + 33.3 wt% SiC	195.1 ± 3.9
50 wt% Ni + 20 wt% Ti + 30 wt% SiC	244.4 ± 16.0
80 wt% Ni + 15 wt% Ti + 5 wt% SiC	312.8 ± 12.9

Conclusions

Laser alloying of aluminium AA1200 was successfully performed with an Nd:YAG laser using Ni, Ti and SiC powders in various composition mixtures. Metal matrix composites and intermetallic phases were formed in the surface of the aluminium AA1200 metal. The formation of the intermetallic phases resulted in an improved surface hardness which was found to increase with increasing Ni content. The highest hardness was achieved when laser alloying with Ni powders only. This hardness was 32 times that of the pure aluminium. When laser alloying with Ni, Ti and SiC simultaneously, a maximum hardness increase of 13 times that of pure aluminium was achieved when alloying with a powder mixture of 80 wt% Ni + 15 wt% Ti + 5 wt% SiC. The grain morphology of the intermetallic and metal matrix composite phases as well as the aluminium mean free path influenced the hardness. Dense, equiaxed dendritic phases and small mean free paths led to high hardness values while the needle-like and platelet phases with large mean free paths produced low hardness values.

References

[1] Riabkina-Fishman, M., & Zahavi, J. (1996). *Appl. Surf. Sci.*, *106*, 263.
[2] Ravi, N., Sastikumar, D., Subramanian, N., Nath, A. K., & Masilamani, V. (2000). *Mater. Manuf. Processes*, *15*, 395.
[3] Bysakh, S., Mitra, S. K., Phanikumar, G., Mazumder, J., Dutta, P., & Chattopadhyay, K. (2003). *Metall. Mater. Trans. A 34*, 2621.
[4] Selvan, J. S, Soundararajan, G., & Subramanian, K. (2000). *Surf. Coat. Technol.*, *124*, 117.
[5] Bao, C. M., Dahlborg, U., Adkins, N., & Calvo-Dahlborg, M. (2009). *J. Alloys Compd.*, *481*, 199.
[6] Watkins, K. G., MacMahon, M. A., & Steen, W. M. (1997). *Mater. Sci. Eng. A*, *231*, 55.
[7] Wendt, U., Settegast, S., & Grodrian, I. U. (2003). *J. Mater. Sci. Lett.*, *22*, 1319.
[8] Man, H. C., Zhang, S., & Cheng, F. T. (2007). *Mater. Lett.*, *61*, 4058.
[9] Mabhali, L., Pityana, S., & Rampedi, L. (2008). *Microsc. Soc. South. Af. Proc.*, *38*, 19.
[10] Hu, C., & Baker, T. N. (1997). *J. Mater. Sci.*, *32*, 5047.
[11] Walter, D., & Karyasa, I. W. (2005). *J. Chin. Chem. Soc.*, *52*, 873.
[12] Su, R., & Lei, Y. (2008). *Mater. Lett.*, *62*, 3272.

[13] Anandkumar, R., Almeida, A., Colaço, R., Vilar, R., Ocelík, V., & De Hosson, J. Th. M. (2007). *Surf. Coat. Technol.*, *201*, 9497.
[14] Xu, X., Han, J., Li, Y., & Liu, L. (2006). *J. Ceram. Processing Res.*, *7*, 167.
[15] Leòn, C. A., & Drew, R. A. L. (2002). *Compos. A*, *33*, 1429.
[16] Hashim, J., Looney, L., & Hashmi, M. S. J. (2001). *J. Mater. Processes Technol.*, *119*, 324.
[17] Kloosterman, A. B., Kooi, B. J., & De Hosson, J. Th. M. (1998). *Acta Mater.*, *46*, 6205.
[18] Pei, Y. T., Ocelik, V., & De Hosson, J. Th. M. (2002). *Acta Mater.*, *50*, 2035.
[19] Gu, W. L., Yan, C. K., & Zhou, Y. C. (2003). *Scripta Mater.*, *49*, 1075.
[20] Viala, J. C., Peillon, N., Bosset, F., & Bouix, J. (1997). *J. Mater. Sci. Eng. A*, *229*, 95.
[21] Kooi, B.J, Kabel, M., Kloosterman, A. B., & De Hosson, J. Th. M. (1999). *Acta Mater.*, *47*, 3105.
[22] Qin, F., Fan, T., & Zhang, D. (2008). *Metall. Mater. Trans. A*, *40*, 462.
[23] Rao, K. P., & Zhou, J. B. (2004). *J. Mater. Sci.*, *39*, 5471.
[24] Li, S., Zhou, Y., & Duan, H. (2002). *J. Mater. Sci.*, *37*, 2575.
[25] Man, H. C., Zhang, S., Cheng, F. T., & Yue, T. M. (2002). *Scripta Mater.*, *46*, 229.
[26] Man, H. C., Zhang, S., Yue, T. M., & Cheng, F. T. (2001). *Surf. Coat. Technol.*, *148*, 136.
[27] Guan, Q. L., Wang, H. Y., Li, S. L., Wang, W. N., Lü, S. J., & Jiang, Q. C. (2009). *Mater. Chem. Phys.*, *114*, 709.
[28] Froes, F. H., Suryanarayana, C., & Eliezer, D. (1991). *ISIJ Int.*, *31*, 1248.
[29] Brytan, Z., Bonek, M., & Dobrzański, L. A. (2010). *J. Achievements Mater. Manuf. Eng.*, *40*, 70.